Digest Journal of Nanomaterials and Biostructures Vol. 8, No. 1, January - March 2013, p. 177 - 185

FRACTURE OF FEMUR: SIMULATION AND PHOTOELASTICITY ANALYSIS

JAIME HORTA[a], ANA LEONOR RIVERA[b], AGUSTIN DE LA ISLA[a], ADRIAN OSKAM[b], VICTOR M. CASTANO[b*]
[a]*Universidad Autonoma de Queretaro, Campus Cerro de las Campanas, Santiago de Queretaro, Queretaro 76010, México*
[b]*Centro de Física Aplicada y Tecnologia Avanzada, U.N.A.M., Boulevard Juriquilla 3001, Santiago de Querétaro, Querétaro 76230, México*

Bones, particularly long ones, are among the most fascinating and intriguing materials, not only because of the complicated structure, but also because of their mechanical behavior, which is still not completely understood.Finite Element computer simulations of the modal behaviour of human femur were compared to experimental results of the resonance frequencies of actual bones, indicating that the details of the boundary conditions and the cross section are key if a better understanding of the mechanical properties of bones is to be achieved. Fractures do not present a defined path, neither when they first appear, nor in their evolution along the cross section, but rather show a totally irregular section. FEM simulations point out the need of taking into account possible changes in cross section and boundary conditions of the epiphysis of femoral human bones. Finite Element computer simulations of the modal behaviour of human femur were compared to experimental results of the resonance frequencies of actual bones, indicating that the details of the boundary conditions and the cross section are key if a better understanding of the mechanical properties of bones is to be achieved. The stress distribution, in both epiphysis and diaphysis femoral regions, was determined by photoelasticity experiments.

(Received November 12, 2012; Accepted January 7, 2013)

Keywords: Femur; Diaphysis; Epiphysis; Modal analysis; Finite element method; Photoelasticity

1. Background

Bones, particularly long ones, are among the most fascinating and intriguing materials, not only because of the complicated structure, but also because of their mechanical behaviour [1-5] and a number of recent studies have pointed out some of their unique features, especially during fracture under severe mechanical loading [5,6]. Indeed, the mechanical response of long bones depends on many physical and biochemical variables, yet to be understood. For instance, the bone in situ stands a temperature of 37.0 ^{o}C and a high humidity environment, which influences the weak chemical bonding (hydrogen-like) of these materials. It has also been observed that bone adapts to the applied loads by minimizing possible damages, through yet unknown physicochemical mechanisms [3,4]. Of great theoretical and practical importance in bone studies are the questions related with its natural welding and consolidation process after fracture, in addition to bone remodelling and growth mechanisms[3].

Given the complexity of the bone spatial structure, detailed analysis of its mechanical properties pose a serious challenge, beginning with the varying cross section of a long bone, which makes standard stress-strain studies in a typical Instron-type machine unreliable, following by the fact that the graded porosity of calcified tissue make the characterization of plastic, plaster or

*Corresponding author: castano@fata.unam.mx

metal mimics of bones, a crude approximation to the actual situation. In fact, more that simple numerical figures of the maximum strain a bone can stand, for example, details on the stress distribution during mechanical loading would enlighten the situation. In this regard, photoelasticity offers an attractive approach to the problem, since its provides a fairly accurate picture of stress distribution even around abrupt discontinuities in a material[6]. In spite of being a tool for determining the critical stress points in a material and also being often used for determining stress concentration factors in irregular geometries, photoelastic studies of actual bone are relatively scarce in the literature and most of the available references deal with teeth[7], given the obvious relevance to orthodontics.

On the other hand, computer simulation and design in engineering has witnessed a tremendous advance in the last few decades, due to the availability of powerful Finite Element Method (FEM) software packages[8-12] and some valuable attempts to understand, via the use of these computing tools, the biomechanics of long bones can be found in the literature [11-15].

Accordingly, in this present article we report a combined approach towards the characterization of the behaviour of human femur by using FEM simulations[12-14] along with photoelasticity analysis, aiming to a better understanding of which are the key parameters to consider for the fracture of a real long bone. Although FEM has been utilized successfully in recent years for many biomechanical applications[13-17], including topological optimization of prosthesis[15], its use for understanding the mechanical properties of the bone itself has been more limited. The combination of photoelasticity and FEM is certainly a unique approach. We focus our analysis on the evaluation of frequency variations versus depth bone crack as a measure of the rehabilitation of fractured bone.

2. Consolidation process of fractured bones

According to Continuum Mechanics, the equations of local conservation of the mass are expressed by

$$\dot{\rho} + \rho div\, v = 0 \quad ; \quad \rho' + div\,(\rho v) = 0 \tag{1}$$

being:

$\dot{\rho}$: material time derivative of the density spatial field;

ρ' : spatial derivative of density field

v: velocity field

The structure of a bone is that of a composite material with two essential phases: a solid phase constituted by fibres of collagen and made up of calcium, and a soft phase composed by chanels and interstices occupied by marrow. Volum relationship of voids V_P with respect to the total volume V_T is the parameter $n = V_P / V_T$. This relationship as a function of the density is also expressed as: $n = 1 - \rho / \rho_o$. Here, ρ_o is the reference density. Introducing the tensor gradient of deformation J (and Jacobean matrix [J]), we can write the following expression:

$$n = 1 - \frac{1}{det[J]} \tag{2}$$

Here:

J: Second order Tensor = Grad f

f: deformation function

Involving equations (1) and (2) we have:

$$\frac{\partial \rho}{\partial t} + \text{div}\,[(1 - n)\rho_o v] = 0 \tag{3}$$

Jacobi proposed an adjusted expression:

$$\frac{\partial \rho}{\partial t} = \left(\frac{\partial \rho}{\partial t}\right) S_v \rho_o \quad (4)$$

So the behaviour of bone density with time involves the velocity of superficial remodelling of the bone which include growth and consolidation. Parameter S_v is the available surface for unit of bone volume and depends of the porosity. Under isotropic behaviour the Stress Tensor S is expressed as follow:

$$S = 2\mu\, E + \lambda\, tr\,(E) I \quad (5)$$

Here:
E: Tensor of infinitesimal deformations;
Tr: Operator Traza
I: Identity Tensor; μ, λ : Lame constants
Next tables resumes the data used to realize the analysis

Table 1. Parameters for healthy bone.

Bone without Fracture			
Material	E (MPa)	Poisson Ratio ν	Density ρ (T/m^3)
Marrow	--------	0.45	900
Compact Bone	15000	0.32	1952
Trabecular Bone	3177	0.32	1200

Table 2. Parameters for fractured bond and consolidation process

Bone with Fracture and consolidation process			
Material	E (MPa)	Poisson Ratio ν	Density ρ (T/m^3)
Marrow	--------	0.45	900
Compact Bone (according to equations 3&4)	15000 10000 5000 1000	0.32 0.32 0.32 0.32	1952 1720 1385 837

3. Modal analysis

A) Finite element simulation
The governing equations for undamped modal analysis is[9]:

$$[M]\{\ddot{U}\} + [K]\{U\} = \{0\} \quad (6)$$

Here: [M] the mass matrix, [K] Stiffness matrix, {U} displacement vector.

The boundary conditions, as well as the specific finite element applied are shown in Fig 1. The technical details of the FEM simulation, using the ANSYS package[10] were provided in a separate publication of this series[12]. For the simulations the bone density was taken according to tables 1 & 2 and depending of bone case. One is able to determine the values of ρ, and ν when varying E, as has been reported by the present authors elsewhere[12]. Figure 1 shows the boundary conditions as well the Master Degree of Freedom used inside of the analysis.

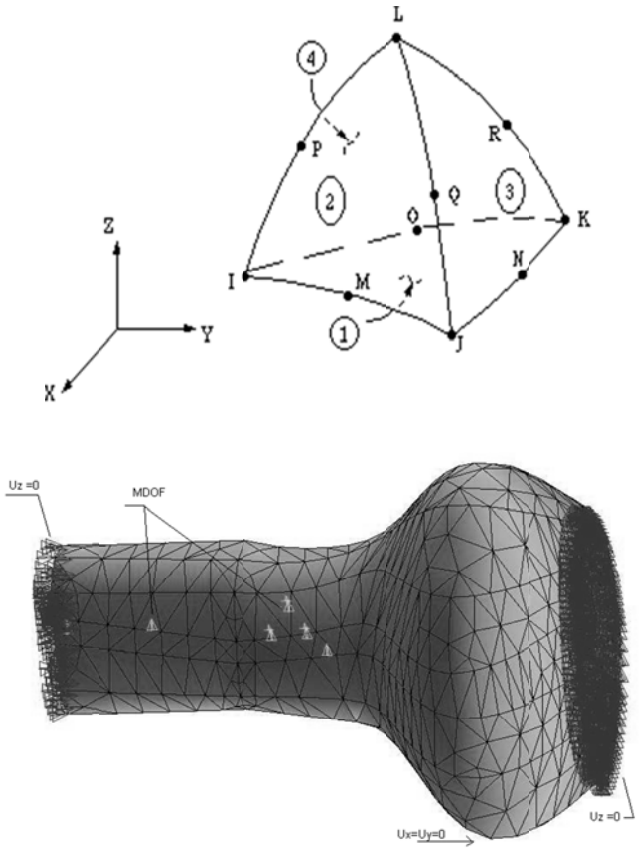

Fig. 1.Boundary conditions and finite element utilized in the simulations.

B) Experimental modal analysis

Figure 2 shows schematically the experimental setup for the modal analysis of a human femur. The procedure has consisted in the application of an excitation force on some selected points using an impact hammer and measuring the bone frequency response. Figure 3 shows the amplitude forces as well the peaks resonant frequencies.

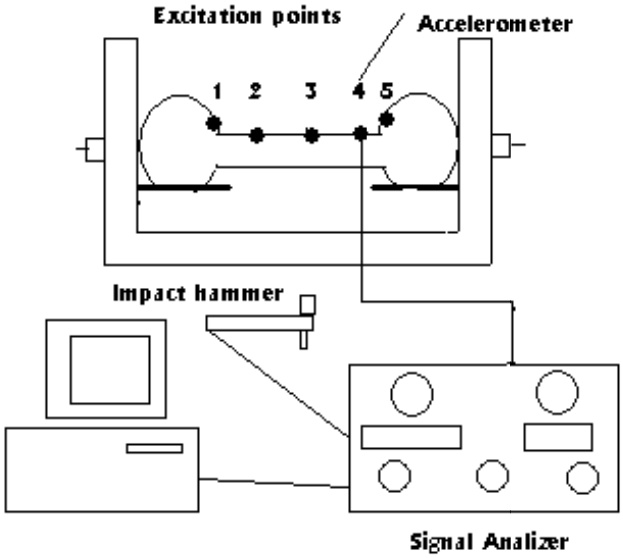

Fig. 2.Experimental setup of the experimental modal analysis of the bone.

4. Photoelasticity setup

A special, strain-sensitive plastic coating is first bonded to an actual human bone (femur). Since the photoelastic coating is intimately and uniformly bonded to the surface of the bone, the strains in the bone are faithfully transmitted to the coating. The strains in the coating produce proportional optical effects, which appear as isochromatic fringes when viewed with a reflection polariscope. In the full-fields pictures the pattern of isochromatic fringes when the bone is subjected, along the cross section, to a load of 80 kg.

5. Results and discussion

Fractures do not present a defined path, neither when they first appear, nor in their evolution along the cross section, but rather show a totally irregular section. To account for this in the FEM ANSYS simulation, an irregular section at the central part of the bone, with an average thickness of 2.0 cm, was chosen, then the total average thickness of the consolidation zone will be 4 cm.

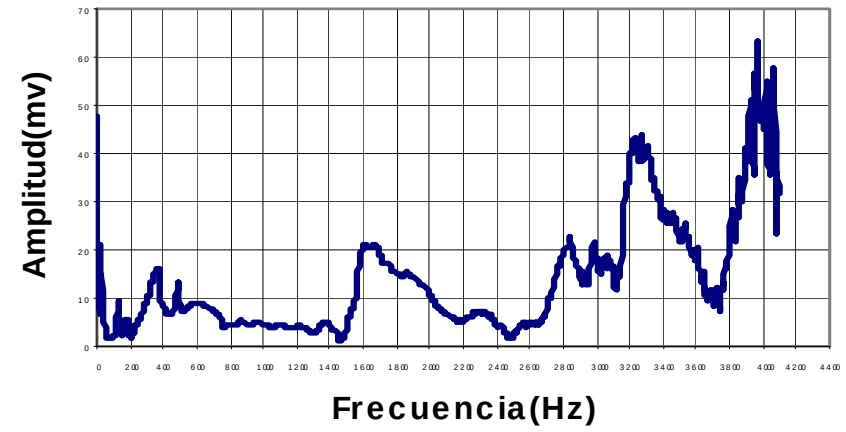

a

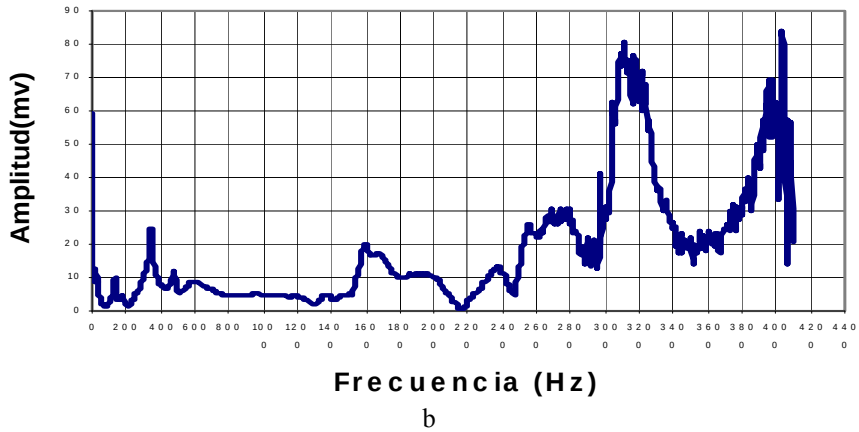

b

Fig. 3.Spectra of the bone response for cracks of: a) 0.8 cm and b) 1.6 cm.

Typical experimental spectra are displayed in Figures 3(a) and 3(b), corresponding to crack depths of 0.8 cm and 1.6 cm, respectively, excited at point 1 (see Figure 2), along with the ANSYS simulations. As can be observed in Figure 4, which contains plots of both simulated and experimental resonance frequencies, for the first two modes there exist significant differences between simulated and experimental resonance frequencies. This may be due to the presence of

inner fractures in the inferior central area therefore. When this fracture is evolving, discontinuities and concentrations of stresses would be generated. There exist various procedures to evaluate this behaviour through the so-called J integral the J around the crack[8]. Diverse authors propose different methods to evaluate the close-open effect of the crack, although our simulation is based on the proper modification of the boundary conditions from the centre of the span that allows the natural evolution of the crack, as shown in Figure 5, which allows to adjust the resonance frequencies to the experimental ones. Six Master's degrees of freedom are chosen one of them in the centre of the span where the fundamental frequency of the bone is presented. Biomechanical[13] and clinical studies across age and sex of femoral diaphysis[14] show that a the increase in fracture rates may be related to a decrease in bone mass with a presumed loss of strength. This decrease may possibly be compensated for by changes in cross-sectional geometry, which supports the approach suggested here.

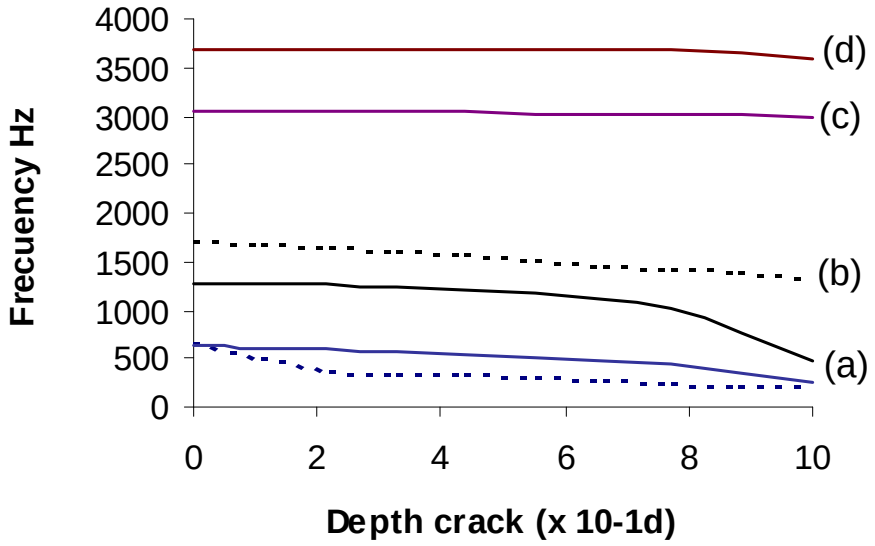

Fig. 4.Resonance frequency vs. evolution of the crack.(a), (b): experimental (dashed lines) and analytical results (full lines) for first and second modes; (c), (d): analytical, for third and forth modes.

The photoelastic patterns appear as a series of successive coloured bands in which each band represents a different degree of birefringence, fringe order (and strain level), corresponding to strain gradients and the overall strain distribution, including the identification of overstressed and understressed areas. The fringe orders observed in photoelastic coatings are proportional to the difference between the principal strains in the coating (and in the surface of the test part). This simple linear relationship can be expressed as follows:

$$\varepsilon_x - \varepsilon_y = Nf \tag{7}$$

where:

εx , εx = principal strains; N = fringe order.

$f = \frac{\lambda}{2tK}$. Fringe value of coating

λ = wavelength (in white light, 22.7x10-6in or 575nm)

t = thickness of coating.

K= strain optical coefficient of coating.

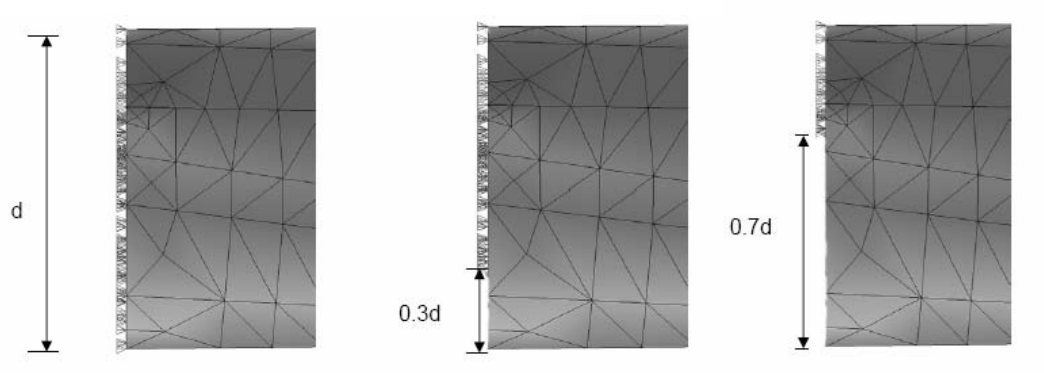

Fig. 5. Adjusted boundary conditions fro the FEM simulation: (a) no crack; (b) length crack = 0.3d; (c) length crack = 0.7 d

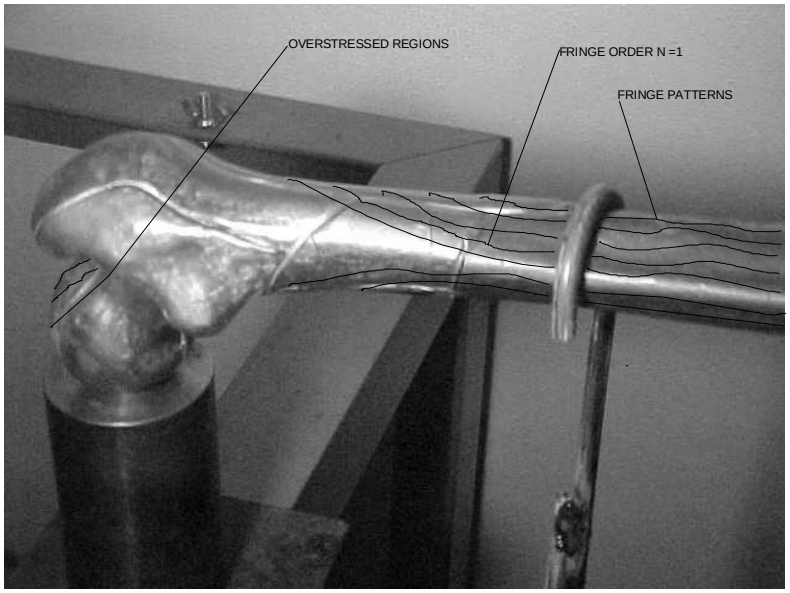

a

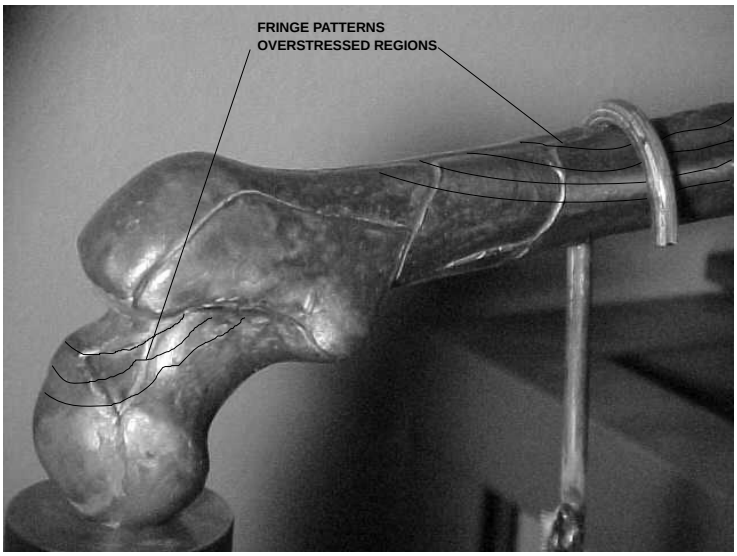

b

Fig. 6. Areas of stress concentration in: a) the diaphysis of a human femur and b) the epiphysis of a human femur.

Figures 6(a) and 6(b) show photographs of the stress distribution, as revealed by the photoelasticity experiments, of the diaphysis and epiphysis of the femur, respectively. Again, as in the FEM simulations, the stress distribution is associated to the boundary conditions, including slight changes in cross section, of the bone. Biomechanical models of the stress distribution in bones, based upon clinical studies[13] have indicated the femoral neck width and the resultant hip force have important influence on shear stress distribution.

6. Concluding remarks

Our FEM simulations point out the need of taking into account possible changes in cross section and boundary conditions of the epiphysis of femoral human bones, in agreement with clinical studies that indicate that bone tissue was redistributed when a reduction in cortical area was detected, specially as a function of age[14].

The photoelastic results also support this position and relatively recent clinical studies indicate that even unfavourable high values of the hip force can be compensated by larger collum-diaphysis angle and wider femoral neck[13, 17]. As those clinical analysis conclude, these studies could be used, provided a larger series of patients is available, to even predict the value of the shear stress for different clinical outcomes.

Acknowledgements

The authors are indebted to Prof. Alfredo Olivares and to Dr. Guillermo Silva Pineda and Dr. Luis Reyes Araiza for their support in the experimental phase of the present work.

References

[1] C.A. Regirer and A.A. Shtein (Editors), Modern Problems in Biomechanics, Zinatne Pub., Riga (1985)
[3] D. R. Carter, Mechanics loading history and skeletal biology, J. Biomechanics **20**, 1095-1109 (1987).
[4] C.E. Oxnard, Thought on bone biomechanics, Folia Primatologica **75**, 4 (2004)
[5] R. Solares, F. Villegas, J. Guerrero A. Olivares and G. Herrera, Biomecánica del Peroné, Revista Prensa Médica Mexicana, No. 11-12, Mexico City (1974)
[6] C. R. Jacobs, Numerical Simulation of bones adaptation to mechanical loading, Ph.D. Thesis, Stanford University (1994)
[7] J. F. Orr and J. B. Finlay, Optical measurement methods in biomechanics, Springer, New York (1996)
[8] A. Asundi, A strain gauge and photoelastic analysis of in vivo strain and in vitro stress distribution in human dental supporting structures, Archives of Oral Biology **45**, 543-550 (2000)
[9] M. Gurtin, An introduction to continuum mechanics, Academic Press, New York City (1991)
[10] R. Cook, D. Malkus and M. Plesha, Concepts and applications of finite element analysis, John Wiley, New York City (1989)
[11] SAS IP, Inc. (Swanson Analysis Systems, Incorporated), "Expanded ANSYS workbook for Revision 5.2" (1996
[12] J.M. García and M. Doblaré, Simulación por elementos finitos del problema de remodelación ósea interna. Aplicación a la extremidad proximal del fémur, Memorias del Congreso Internacional de Métodos Numéricos en Ingeniería, SEMNI, Spain (1999)
[13] J. Horta, A.L. Rivera and V.M. Castaño, Modal behavior of bones during fracture, Comp. Meth. in Biomech. and Biomed. Eng. **13**, 91 (2010)
[14] B. Mavcic, M. Kryzancic, O. Zupanc, A. Iglic and V. Kralj-Iglic, Biomechanical model of the shear stress distribution in the femoral neck, Bull. Appl. Mech. **4**, 225-230 (2005)
[15] M.S. Stein, C.D.L. Thomas, S.A. Feik, J.D. Wark and J.G. Clement, Bone size and mechanics

at the femoral diaphysis across age and sex, J. Biomech. **31**, 1101-1110 (1998)
[32] M. Fraldi, L. Esposito, G. Perrella , A. Cutolo and S. C. Cowin, Topological optimization in hip prosthesis design, Biomech. Model. Mechanobiol. **9**, 389–402 (2010)
[33] S. Gross and E.W. Abel, A finite element analysis of hollow stemmed hip prostheses as a means of reducing stress shielding of the femur, J. Biomech. **34**, 995–1003 (2011)
[34] M. Ruess, D. Tal, N. Trabelsi, Z., Yosibash and E. Rank, The finite cell method for bone simulations: verification and validation, Biomech. Model. Mechanobiol. **11**, 425–437 (2012).

Authors' Contributions

J. H. y A. R.: Simulation by Finite Method.
A. O.: Experimental Design of Photoelasticity Tests.
A. I. Biomechanical and Biological Design.
V. C.: Modeling and Theoretical Background.